Journal of Solid State Chemistry 183 (2010) 1545–1549

Contents lists available at ScienceDirect

Journal of Solid State Chemistry

journal homepage: www.elsevier.com/locate/jssc

Calcium-doped ceria/titanate tabular functional nanocomposite by layer-by-layer coating method

Xiang W. Liu *, M.K. Devaraju, Shu Yin, Tsugio Sato *

Institute of Multidisciplinary Research for Advanced Materials, Tohoku University, 980-8577 Suita, Japan

ARTICLE INFO

Article history:
Received 25 January 2010
Received in revised form
26 April 2010
Accepted 27 April 2010
Available online 13 May 2010

Keywords:
Tabular titanate
Nanocomposite
UV shielding
Layer by layer
Coating

ABSTRACT

Ca-doped ceria (CDC)/tabular titanate ($K_{0.8}Li_{0.27}Ti_{1.73}O_4$, TT) UV-shielding functional nanocomposite with fairly uniform CDC coating layers was prepared through a polyelectrolyte-associated layer-by-layer (LbL) coating method. TT with lepidocrocite-like layered structure was used as the substrate, poly (diallyldimethylammonium chloride) (PDDA) was used as a coupling agent, CDC nanoparticles were used as the main UV-shielding component. CDC/TT nanocomposites with various coating layers of CDC were obtained through a multistep coating process. The phases were studied by X-ray diffraction. The morphology and coating quality were studied by scanning electron microscopy and element mapping of energy dispersive X-ray analysis. The oxidation catalytic activity, UV-shielding ability and using comfort were characterized by Rancimat test, UV-vis spectra and dynamic friction test, respectively. CDC/TT nanocomposites with low oxidation catalytic activity, high UV-shielding ability and good using comfort were finally obtained.

1. Introduction

With the identification of serious damages caused by ultraviolet (UV) radiation from sunlight, various UV-shielding materials such as zinc oxide and titania, have been developed and widely used in personal products, but the reactive oxygen species caused by their high photocatalytic activity have raised safety concerns [1,2]. In response to that, Ca-doped CeO_2 (CDC) nanoparticles, as a promising UV-shielding candidate with lower photocatalytic activity, lower oxidation catalytic activity and lower refractive index, have been formerly synthesized and studied by our group [3,4]. However, the using comfort and covering capability on skin of CDC were not satisfying due to their agglomerations [5]. In order to solve this problem CDC/tabular titanate ($K_{0.8}Li_{0.27}Ti_{1.73}O_4$, TT) nanocomposites have been tentatively prepared [6,7]. As expected, the using comfort of CDC nanoparticles was greatly improved by tabular TT. Unfortunately, the lower K_{sp} value of calcium hydroxide caused an irreconcilable conflict between the pH value of solution and doping concentration of Ca^{2+} in CDC in co-precipitation method. Low pH will decrease the doping concentration of Ca^{2+} in CDC and consequently enhance the oxidation catalytic activity [6]. In order to effectively depress the oxidation catalytic activity the CDC nanoparticles have to be prepared above pH 11.0, while both TT and CDC particles are negatively charged above pH 6.5, which is seriously adverse to the adhesion of CDC on TT. On the other hand, the electrostatic layer-by-layer (LbL) coating method, which was initially developed by Decher in 1991 for producing thin polymer films by a polyelectrolyte multilayer coating route [8], has been paid much attention. Now, polyelectrolyte multilayer coating technique has been widely extended to other applications such as carbon nano-tube coating [9], anticorrosion protection coating [10,11], incorporation of other charged species such as proteins [12,13], gene delivery [14], cell carrier [15] and small inorganic particles [16,17]. This method is strongly dependent on the surface charge character of material. Inspired by this method, CDC/TT nanocomposites were prepared utilizing the electrostatic attraction between CDC and TT particles by using a poly (diallyldimethylammonium chloride) (PDDA)-associated LbL coating route at high pH value. PDDA, as a positively charged polyelectrolyte, was used as a coupling agent to adjust the surface charge of particles. The successful surface charge reversal of TT was confirmed by zeta-potential measurement. This method was proved to be capable of resolving the conflict between pH and doping concentrations of Ca^{2+} in CDC and more economical and eco-friendly.

2. Experimental

2.1. Materials

All the chemical reagents: $CeCl_3 \cdot 7H_2O$ (A.R., Kanto Chemical Co., INC.), $CaCl_2 \cdot 2H_2O$ (A.R., Kanto Chemical Co., INC.), hydrogen

* Corresponding author.
E-mail addresses: lxwluck@gmail.com, lxwluck@163.com, xwliu@ri.ncvc.go.jp (X.W. Liu).

0022-4596/$ - see front matter © 2010 Elsevier Inc. All rights reserved.
doi:10.1016/j.jssc.2010.04.040

peroxide solution (H_2O_2, 30%, Santoku Chemical Industries Co. Ltd.), poly (diallyldimethylammonium chloride) (PDDA, MW: 100,000–200,000, 20% solution in H_2O, Sigma-Aldrich, USA) were used without further purification.

2.2. Preparation of CDC sol

The experiment was carried out in a water bath temperature control system and the temperature was maintained at 40 °C. The pH value was maintained at ca. 11.5. Certain $CeCl_3$ (0.08 M)–$CaCl_2$ (0.02 M) solution and sodium hydroxide solution (0.1 M) were simultaneously dropped into a beaker with a speed of 30 ml/h under stirring and the mixture gradually turned into light violet color. After that, certain 0.2 M H_2O_2 aqueous solution was added and the mixture finally became yellow in color.

2.3. Synthesis of CDC/TT nanocomposites

Typically, 1 g TT was dispersed into 50 ml PDDA aqueous solution, the pH value of which was adjusted to 10–11 by sodium hydroxide solution under stirring. After 30 min the TT particles were separated by centrifugation and carefully washed with buffer solution several times to remove the extra PDDA, then the zeta-potential tendency versus pH of them was measured. After that the TT/PDDA particles were dispersed into 20 ml water and consequently dropped into the above prepared CDC sol with a speed of 50 ml/h, after keeping stirring for 1 h the slurry was filtrated and washed 3 times alternatively with water and ethanol. Then, the obtained CDC/PDDA/TT particles were treated again by PDDA solution. As shown in the flow sheet (Fig. 1), by repeating this charge reversal and coating cycle TT coated with multilayers of PDDA and CDC were obtained. After removing the organic part by calcination at 700 °C for 1 h, CDC/TT nanocomposites with various CDC concentrations were finally obtained. Hereafter, the samples are denoted as CDC/TT/*x*% (*x*: the mass percent of CDC). The volumes of $CeCl_3$ (0.08 M)–$CaCl_2$ (0.02 M) solution, coating times, theoretical and real concentrations of CDC for various CDC/TT nanocomposites are listed out in Table 1.

2.5. Characterization

FE-SEM and EDX: The morphology of CDC/TT nanocomposites and the size of CDC nanoparticles were observed by a field-emission scanning electron microscope (FE-SEM, Hitachi, S-4800). The Ca^{2+} content in CDC and elementary distribution pattern were measured by an energy dispersive X-ray spectrometer (EDX-800HS, Shimadzu).

Rancimat test: The catalytic ability for oxidation of organic material was measured by Rancimat method [3] using cosmetic grade castor oil as an oxidized material. The catalytic ability of sample was determined by the induction time which is defined as the time at which the conductivity of water obviously begins to increase.

Dynamic friction measurement: The using comfort of samples was evaluated by measuring their dynamic friction coefficients using a friction tester (Katotech, KES-SE) which employs a piano wire as a friction sensor and the artificial leather as the substrate.

Table 1
Volumes of solution of $CeCl_3$ (0.08 M)–$CaCl_2$ (0.02 M), coating times, theoretical and real concentrations of CDC for various CDC/TT nanocomposites.

Sample	$CeCl_3$–$CaCl_2$/ml	Coating times	Theoretical *x*%	Real *x*%
CDC/TT/17.8%	1.67	1	20	17.8
CDC/TT/32.6%	2.10	2	36	32.6
CDC/TT/45.1%	2.50	3	48	45.1
CDC/TT/52.8%	2.75	4	57	52.8
CDC/TT/60.0%	2.90	5	64	60.0

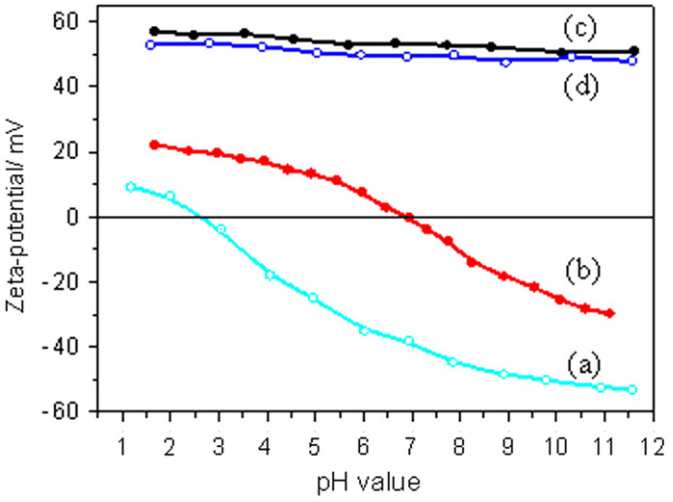

Fig. 2. The zeta-potential curves of (a) TT substrate; (b) CDC sol; (c) PDDA/TT after charge reversal treatment; (d) PDDA/CDC/PDDA/TT particles.

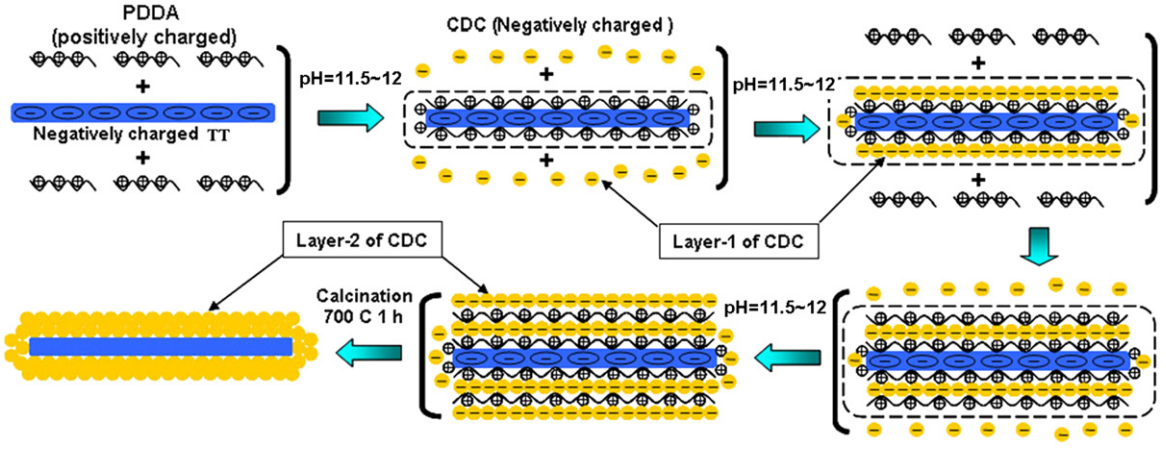

Fig. 1. The flow sheet for the preparation of CDC/TT nanocomposite by LbL multistep coating method.

The dynamic friction coefficients of artificial leather before and after being applied various sample powders on were measured and consequently the dynamic friction coefficient ratios of samples were figured out.

UV-vis transmittance spectra: The UV-shielding ability of samples was evaluated by measuring the transmittance spectra of thin films uniformly dispersed the sample powders with an UV-Vis spectrophotometer (Shimadzu, UV-2450).

3. Results and discussion

3.1. The synthesis of CDC/TT nanocomposites

According to the theory for the adsorption of linear flexible polyelectrolytes presented by Van der Schee and Lyklema [18], the electrostatic contributions to the free energy directly affect the concentration profile and the strong repulsion between the segments of a polyion leads to a very thin adsorbed layers, so the adsorbed amount and thickness of adsorbed layer can be increased through the screening of repulsion by salt adding. Without salt the polyelectrolyte chains are almost oriented flat and parallel to the substrate, but with higher salt concentration the chains will coil due to the screening of charges on the segments [18,19]. In our case, large amount of PDDA might adversely affect the product properties such as color, transparency of visible light and adhesion strength between CDC and TT particles, so additional salt was not used at first and we found that the charge reversion was successfully reached by this simple method. The concentration effect of PDDA on charge reversal extent was investigated and optimum concentration of PDDA was determined as 0.05 g/l. As shown in Fig. 2, the isoelectric points of TT before treatment by PDDA and CDC sol are ca. 2.6 and 7.0, respectively. The TT particles (PDDA/TT) were positively charged after treatment by PDDA (Fig. 2c), indicating the surface charge reversal of TT particles. After the PDDA/TT particles being coated by CDC nanoparticles they were treated again by PDDA solution, the zeta-potential was confirmed to be positive (Fig. 2d).

3.2. XRD patterns of typical CDC/TT nanocomposites

As shown in Fig. 3, with the increase of CDC concentration of CDC/TT composites the intensity of diffraction peaks of TT substrate, especially the peak along (020) direction, is obviously decreased, but the intensity of diffraction peaks of CDC is gradually increased, which means that with the increase of CDC concentration the coating layer of CDC gradually became more and more complete and compact. This result is also supported by the following SEM observation result.

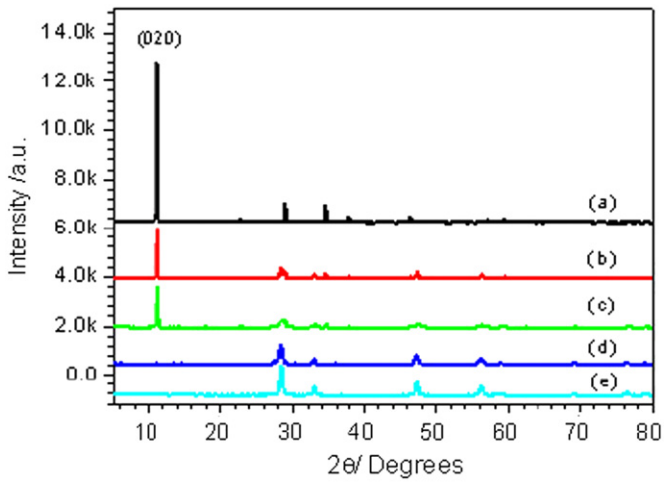

Fig. 3. The XRD patterns of (a) TT substrate; (b) CDC/TT/17.8%; (c) CDC/TT/32.6%; (d) CDC/TT/60%; (e) CDC nanoparticle.

3.3. SEM images and EDX patterns of typical CDC/TT nanocomposites

Considering the effect of the quality of CDC coating layer on the using comfort of the CDC/TT nanocomposites, the optimum content of CDC (ca. 20 mass%) for one layer has been determined in our previous experiment [6].Typical SEM images are shown in Fig. 4. Obvious big agglomerations of CDC can be seen on the surfaces of CDC/TT/20% prepared by co-precipitation method at pH 12.0 (Fig. 4a), indicating the deposition of CDC on TT is not satisfying due to the electrostatic repulsion between them at pH 12.0. In contrast, the surfaces of CDC/TT/17.8% (Fig. 4b) and CDC/TT/60% (Fig. 4e) are smooth and almost no obvious CDC agglomerations; however, some bare spaces among CDC particles can be seen in CDC/TT/17.8% (Fig. 4d), but the covering of CDC/TT/60.0% (Fig. 4f) is complete and the size of CDC nanoparticles is ca. 10–20 nm. In addition, element mapping and quantitative elemental analysis were carried out on the surface of CDC/TT/60.0% (Fig. 4h–k). The EDX mapping patterns show that Ca and Ce are uniformly distributed in the CDC layer (Fig. 4j,k) and the typical EDX spectrum of the selected area is shown in Fig. 4l. The quantitative elemental analysis was carried out on 10 different CDC/TT particles and the average molar ratio of Ce/Ca was ca. 4.0, indicating that the Ca^{2+} was completely doped into CDC nanoparticles. On the other hand, the molar ratios of Ce/Ti varied along with different CDC/TT particles due to the great variation of the thicknesses of TT substrates.

3.4. Oxidation catalytic activity of typical CDC/TT nanocomposite

It was reported that the oxidation catalytic activity of CDC could be greatly depressed by doping with Ca^{2+} which possesses lower valence and larger ionic size (r=0.112 nm) than Ce^{4+} (r=0.097 nm) and stabilizes the fluorite structure of ceria and consequently depress the release of oxygen molecules [20]. According to the solubility limit of calcium in ceria the molar ratio of Ca/Ce was determined as 1/4 [20]. According to the Rancimat test result (Fig. 5) we can see that compared with the samples prepared by co-precipitation method the induction times of all the samples prepared by LbL method are accordingly elongated, so the oxidation catalytic activity of CDC/TT nanocomposites is successfully depressed through this LbL coating method at high pH value, indicating the high concentration doping of Ca^{2+}, which is consistent with the quantitative elemental analysis result.

3.5. Dynamic friction coefficients result of typical CDC/TT nanocomposite

Fig. 6 shows that the dynamic friction coefficient ratio of TT substrate is lower than those of TiO_2 and CDC nanoparticles and the friction coefficient ratio of CDC is greatly decreased through the coupling with TT substrate. All the dynamic friction coefficient ratios of CDC/TT nanocomposites by LbL coating are lower than that of CDC even with a coating concentration of 60 mass%. The dynamic friction coefficient ratio of the CDC/TT/60% by co-precipitation method is larger than that of TT and almost equal to that of CDC, which might be attributed to the poor quality of CDC coating layers caused by agglomerations. But the dynamic friction coefficient ratio of CDC/TT/60% (31.6%) is comparable to that of CDC/TT nanocomposite (30.5%)

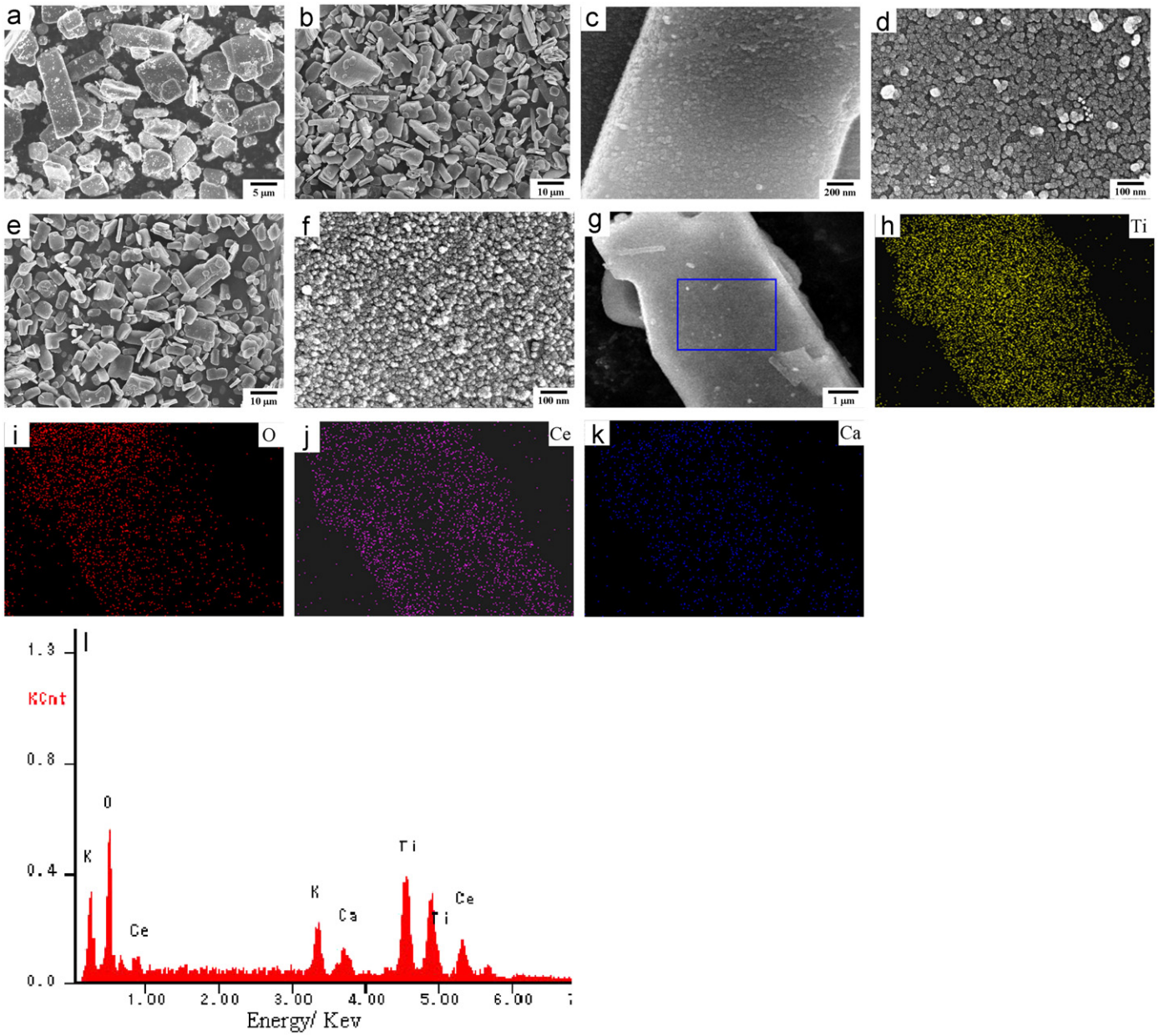

Fig. 4. Typical SEM images of (a) CDC/TT/20% prepared by co-precipitation method; (b)–(d) CDC/TT/17.8%; (e)–(g) CDC/TT/60%; (h)–(k) the elementary mapping patterns of Ti, O, Ce and Ca on the surface of CDC/TT/60%; (l) the typical EDX spectrum of the selected area in image (g).

with similar CDC concentration by sol-gel method. The testing result of dynamic friction coefficient is in good agreement with the SEM observation results which showed that the surface of CDC/TT nanocomposites prepared by LbL coating method was as smooth as that by sol-gel method.

3.6. *UV-vis transmittance spectra of typical CDC/TT nanocomposite*

The UV-vis transmittance spectra of CDC/TT nanocomposites with various CDC contents are shown in Fig. 7. The onsets of absorption of TT and CDC are ca. 330 and 400 nm, respectively. The CDC nanoparticles showed excellent UV-shielding ability and high transparency in visible light region. It is obvious that with the increase of CDC coating quantities the UV-shielding abilities of CDC/TT nanocomposites increased gradually but the transparency in visible light region decreased slightly, which should be attributed to the increase of the thickness of CDC coating layers. It should be pointed out that the transparency located at 280 nm of CDC/TT/17.8% suddenly decreased from 65% (TT substrate) to 28% after one coating, which is almost the same as that of CDC/TT/20% prepared by sol-gel method [6] but is much lower than that of the sample by co-precipitation method with comparative CDC concentration [7]. So the UV-shielding ability is greatly improved by this LbL coating method. In addition, the UV-shielding ability was increased to almost the same level as pure CDC when the concentration of CDC was up to ca. 60 mass% after 5 times coating, which is similar with the result of sol-gel method [6].

4. Conclusions

On the basis of above results, the following conclusions may be drawn. Firstly, the surface charges of TT and CDC/TT particles

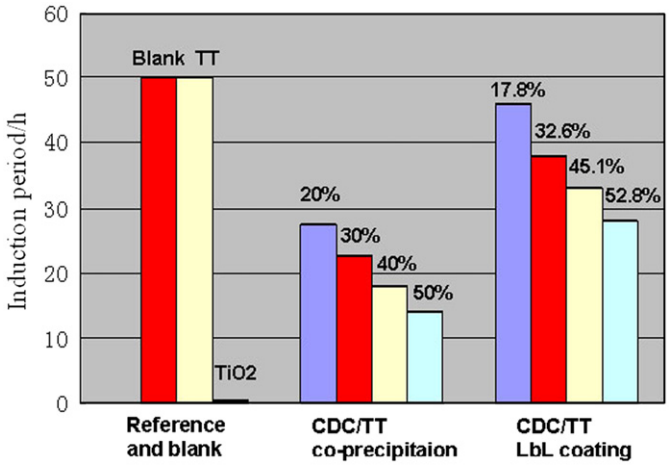

Fig. 5. The induction times obtained by Rancimat test at 120 °C for blank, TT, TiO_2 (Degussa, P25) and CDC/TT nanocomposites with various CDC concentrations by co-precipitation method at pH 6.5 and LbL coating method above pH 11.5.

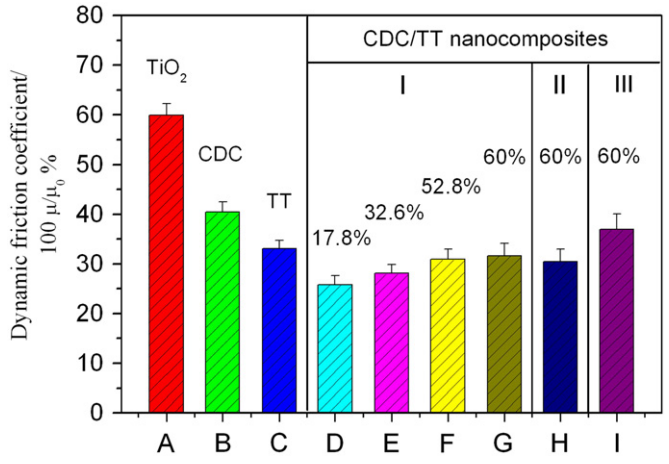

Fig. 6. Dynamic friction coefficients ratios of references and samples. (μ_0: artificial leather without sample; μ: artificial leather applied the sample powder on). (A) TiO_2 (Degussa, P25); (B) CDC nanoparticles; (C) TT substrate; (D) CDC/TT/17.8%; (E) CDC/TT/32.6%; (F) CDC/TT/52.8%; (G) CDC/TT/60%; (H) CDC/TT/60% by co-precipitatoin method.

could be successfully reversed from negative to positive by PDDA, which makes it possible to prepare CDC/TT nanocomposite with uniform CDC coating layers by LbL coating method at high pH, i.e., the LbL coating method overcomes the irreconcilable conflict between the pH value of solution and the doping concentration of Ca^{2+} in CDC. Secondly, the using comfort of CDC nanoparticles is successfully improved through the combination with tabular TT particles. Thirdly, the LbL coating route not only effectively depresses the oxidation catalytic activities but also improves the UV-shielding abilities and using comfort of CDC/TT nanocomposite. As a result, the LbL coating method is proved to be effective for coating of complex micro-particles to fabricate high performance functional materials.

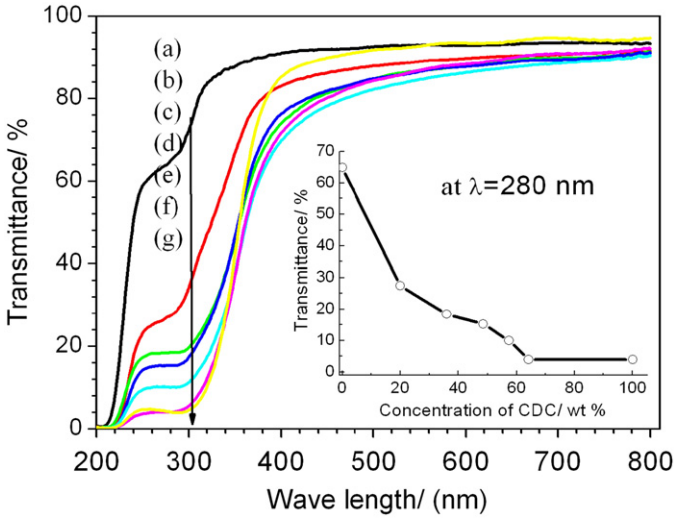

Fig. 7. UV-Vis transmittance spectra of thin films of (a) TT substrate; (b) CDC/TT/17.8%; (c) CDC/TT/32.6%; (d) CDC/TT/45.1%; (e) CDC/TT/52.8%; (f) CDC/TT/60%; (g) CDC nanoparticles.

Acknowledgment

This research was partially supported by the Ministry of Education, Culture, Sports, Science and Technology, Scientific Research of Priority Areas "Panoscopic coating and High Ordered Functions for Rare Earth Materials" and "Special Education and Research Expenses, Post-Silicon Materials and Devices Research Alliance".

References

[1] R. Cai, K. Hashimoto, K. Itoh, Y. Kubota, A. Fujita, Bull. Chem. Soc. Jpn. 64 (1991) 1268.
[2] T.C. Long, N. Saleh, R.D. Tilton, G.V. Lowry, B. Veronesi, Environ. Sci. Technol. 40 (2006) 4346.
[3] S. Yabe, S. Momose, J. Soc. Cosmet. Chem. Jpn. 32 (1998) 372.
[4] R. Li, S. Yabe, M. Yamashita, S. Momose, S. Yoshida, S. Yin, T. Sato, Mater. Chem. Phys. 75 (2002) 39.
[5] T. Sato, A.M. El-toni, S. Yin, T. Kumei, J. Ceram. Soc. Jpn. 115 (10) (2007) 571.
[6] X.W. Liu, J.X. Liu, X.L. Dong, S. Yin, T. Sato, J. Colloid Interface Sci. 336 (2009) 150.
[7] X.W. Liu, S. Yin, T. Sato, Mater. Chem. Phys. 116 (2009) 421.
[8] G. Decher, J.D. Hong, J. Schmitt, Thin Solid Films 210–211 (1992) 831.
[9] B.S. Shim, W. Chen, C. Doty, C.L. Xu, N.A. Kotov, Nano Lett. 8 (2008) 4151.
[10] S.V. Lamaka, D.G. Shchukin, D.V. Andreeva, M.L. Zheludkevich, H. Mohwald, M.G.S. Ferreira, Adv. Funct. Mater. 18 (2008) 3137.
[11] D.V. Andreeva, D. Fix, H. Mohwald, D.G. Shchukin, Adv. Mater. 20 (2008) 2789.
[12] Y.M. Lvov, Z. Lu, J.B. Schenkman, X. Zu, J.F. Rusling, J. Am. Chem. Soc. 120 (1998) 4073.
[13] J. Ji, Q. Tan, D.Z. Fan, F.Y. Sun, M.A. Barbosa, J. Shen, Colloid. Surf. B 34 (2004) 185.
[14] S. Sakai, Y. Yamada, T. Yamaguchi, T. Ciach, K. Kawakami, J. Biomed. Mater. Res. A 88A (2) (2009) 281.
[15] F. Fayazpour, B. Lucas, R.E. Vandenbroucke, S. Derveaux, J. Tavernier, S. Lievens, J. Demeester, S.C. De Smedt, Adv. Funct. Mater. 18 (2008) 2716.
[16] Y. Lvov, K. Ariga, M. Onda, I. Ichinose, T. Kunitake, Langmuir 13 (1997) 6195.
[17] J. Shi, T. Cui, Solid State Electron. 47 (2003) 2085.
[18] H.A. Van der Schee, J. Lyklema, J. Phys. Chem. 88 (1984) 6661.
[19] M.R. Boehmer, O.A. Evers, J.M.H.M. Scheutjens, Macromolecules 23 (1990) 2288.
[20] S. Yabe, M. Yamashita, S. Momose, S. Yoshida, k. Hasegawa, S. Yin, T. Sato, J. Soc. Inorg. Mater. Jpn. 8 (2001) 428.